Available online at www.sciencedirect.com
ScienceDirect
Organic Geochemistry 38 (2007) 1607–1624
Organic Geochemistry
www.elsevier.com/locate/orggeochem

A comparison of biomarker records of northeast African vegetation from lacustrine and marine sediments (ca. 3.40 Ma)

Sarah J. Feakins [a,*], Timothy I. Eglinton [b], Peter B. deMenocal [a]

[a] *Department of Earth and Environmental Sciences, Lamont-Doherty Earth Observatory, Columbia University, Palisades, NY 10964, USA*
[b] *Woods Hole Oceanographic Institution, M.S. 4, Woods Hole, MA 02543, USA*

Received 15 February 2006; received in revised form 6 June 2007; accepted 20 June 2007
Available online 6 July 2007

Abstract

Integrated terrestrial and marine records of northeast African vegetation are needed to provide long high resolution records of environmental variability with established links to specific terrestrial environments. In this study, we compare records of terrestrial vegetation preserved in marine sediments in the Gulf of Aden [Deep Sea Drilling Project (DSDP) Site 231] and an outcrop of lacustrine sediments in the Turkana Basin, Kenya, part of the East African Rift System. We analyzed higher plant biomarkers in sediments from both deposits of known equivalent age, corresponding to a ca. 50–100 ka humid interval prior to the β-Tulu Bor eruption ca. 3.40 Ma, when the Lokochot Lake occupied part of the Turkana Basin. Molecular abundance distributions indicate that long chain *n*-alkanoic acids in marine sediments are the most reliable proxy for terrestrial vegetation (Carbon Preference Index, CPI = 4.5), with more cautious interpretation needed for *n*-alkanes and lacustrine archives. Marine sediments record carbon isotopic variability in terrestrial biomarkers of 2–3‰, roughly equivalent to 20% variability in the C_3/C_4 vegetation contribution. The proportion of C_4 vegetation apparently increased at times of low terrigenous dust input. Terrestrial sediments reveal much larger (2–10‰) shifts in *n*-alkanoic acid $\delta^{13}C$ values. However, molecular abundance and isotopic composition suggest that microbial sources may also contribute fatty acids, contaminating the lacustrine sedimentary record of terrestrial vegetation.

1. Introduction

High resolution, well dated reconstructions of regional and local climate and vegetation change are needed to evaluate the role of environmental variability in hominin evolution. Marine sediments offer relatively long and continuous environmental records capable of resolving orbital-frequency environmental variability over millions of years (e.g. Tiedemann et al., 1994; deMenocal, 1995; Schefuss et al., 2003b). We recently obtained a record of northeast African vegetation variability based on wind blown plant wax biomarker deposits at DSDP Site 231 in the Gulf of Aden (Feakins et al., 2005). This biomarker record indicated large amplitude,

* Corresponding author. Present address: California Institute of Technology, Mail Stop 100-23, Pasadena, CA 91125, USA. Tel.: +1 626 395 1785.
E-mail address: feakins@gps.caltech.edu (S.J. Feakins).

0146-6380/$ - see front matter © 2007 Elsevier Ltd. All rights reserved.
doi:10.1016/j.orggeochem.2007.06.008

orbital timescale (10^4–10^5 year) variability in northeast African vegetation as early as 3.8 Ma. However, since these wind blown sediments integrate environmental conditions across the Horn of Africa and possibly also the Arabian Peninsula, it is not known how the signal relates to specific local conditions, and in particular to environmental conditions in parts of the East African Rift Valley, where many Plio-Pleistocene hominin fossils are preserved. In this study we compare vegetation biomarkers in marine sediments of the Gulf of Aden to biomarkers at a terrestrial site ca. 2000 km away in the Turkana Basin, Kenya, part of the East African Rift System (Fig. 1).

Terrestrial records complement long term reconstructions from marine sediments. They are typically more spatially and temporally fragmented than marine sediments, yielding short lived records of localized environmental conditions (e.g. Lezine, 1991; Huang et al., 1999; Johnson et al., 2002; Feibel, 2003; Bonnefille et al., 2004; Quade et al., 2004; Street-Perrott et al., 2004; Wynn, 2004). In addition, fluvial and lacustrine deposits dominate over wind blown material in most Rift Valley records, presenting a different set of variables and modes of transport that may bias the paleoenvironmental proxy record. In particular, tectonically-driven changes in local hydrography may be difficult to distinguish from changes in climate, given the active tectonic context of the East African Rift Valley (Brown and Feibel, 1988; Partridge et al., 1995; Cohen et al., 1997; Feibel, 1999). A combination of both terrestrial and marine records is therefore needed to enhance our understanding of northeast African paleoenvironments (e.g. Lezine, 1991; Bonnefille et al., 2004; deMenocal, 2004).

Today the Turkana Basin is a closed basin fed by streams from the surrounding highlands (Fig. 1), but for 85% of the Plio-Pleistocene it was an open basin with fluvial drainage (Brown and Feibel, 1988). Tectonic closure of the basin enabled the intermittent formation of large lakes (7500–25,000 km^2) between 4.5–4 Ma and 2 Ma–present, including modern Lake Turkana (Feibel et al.,

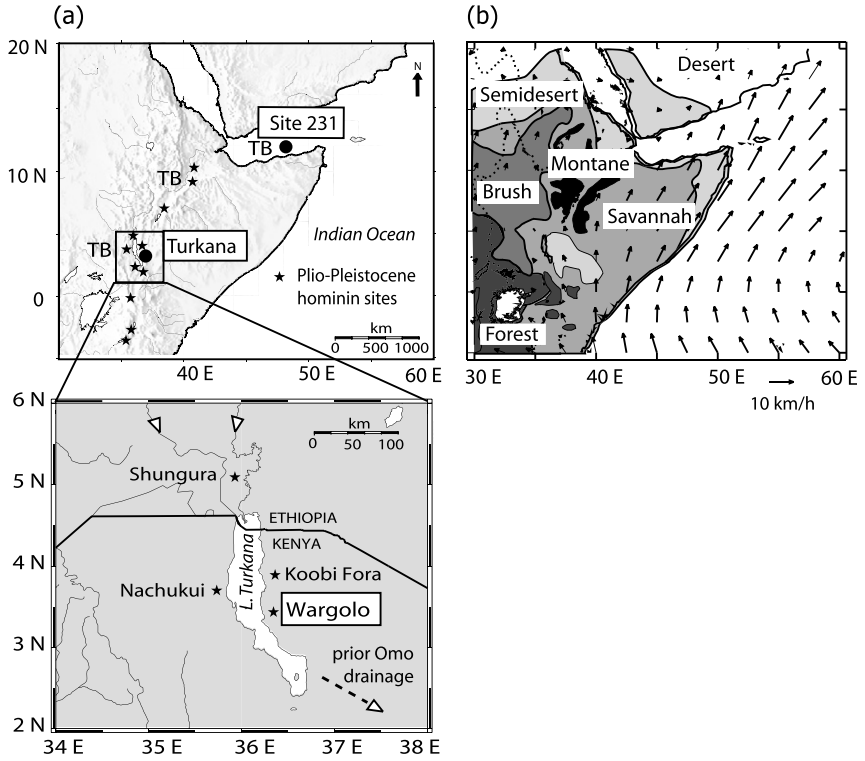

Fig. 1. (a) Locations of DSDP Site 231, Gulf of Aden and Wargolo, Kenya, situated to the east of the present day Lake Turkana (inset). Approximate locations of deposits of the β-Tulu Bor Tuff (TB), major hominin fossil sites (∗) and drainage directions in the Turkana Basin (open arrows) are also shown. (b) Major present day vegetation zones in northeast Africa (White, 1983) and average winds at 1000 hPa (Kalnay et al., 1996) during the period (May–July) of maximum eolian dust production and transport from regional dust source areas (Prospero et al., 2002).

1989). Between 4 and 2 Ma, the open drainage basin did not support large lakes and the ancestral Omo River flowed through the basin, exiting to the southeast (Fig. 1). Ephemeral smaller lakes (~ 2500 km^2) developed between 3.6 and 3.2 Ma, presumably during climatically wet periods (Brown and Feibel, 1988) linked to precession-driven strengthening of precipitation (deMenocal, 1995; Trauth et al., 2001; Tuenter et al., 2003). We investigate biomarker deposition during sedimentation of one such climatically-controlled lakes, the Lokochot Lake (Feibel, 1997).

Lacustrine environments of paleolake Lokochot are recorded in diatomite deposits in the Nachukui and Koobi Fora Formations (Feibel, 1997), including the Wargolo outcrop (~ 3.66°N, 36.25°E) (Fig. 1). To the north, equivalent age sediments record fluvial environments at Area 117, Koobi Fora (~ 4.08°N, 36.28°E) and in the Shungura Formation (5°N, 36°E; de Heinzelin, 1983), indicating that the Lokochot Lake was less extensive (or differently distributed) than the present lake, probably due to increased tectonic segmentation of the basin (Feibel et al., 1991; Feibel, 1997). Subsequent to the termination of the Lokochot Lake period, the β-Tulu Bor Tuff was fluvially deposited over much of the Turkana Basin without much incision of the underlying strata (Feibel, 1997), providing a maximum age for the lacustrine sequence and a means of correlation to the marine sediments of Deep Sea Drilling Program (DSDP) Site 231.

The β-Tulu Bor Tuff is a widespread volcanic ash horizon (Fig. 1) identified at many sites in the Turkana region (Brown and Feibel, 1991). It has been correlated to Hadar, Ethiopia (where it is referred to as the Sidi Hakoma Tuff; Brown, 1982; Walter and Aronson, 1993), and to tephra horizons at DSDP Site 231 in the Gulf of Aden (Sarna-Wojcicki et al., 1985; Brown et al., 1992) and ODP Site 721/722 in the Arabian Sea (deMenocal and Brown, 1999). The age of the β-Tulu Bor Tuff is well constrained at ca. 3.40 Ma, with consistent age estimates at multiple sites (Table 1). This widely correlated and well dated ash layer provides an ideal marker horizon for comparing terrestrial and marine sedimentary records of terrestrial vegetation. We evaluate biomarker reconstructions of vegetation from the Turkana Basin and Gulf of Aden for a 50 ka interval prior to the β-Tulu Bor Tuff as a first step toward integrating terrestrial and marine biomarker records of northeast African environmental conditions.

1.1. Biomarker proxy

We investigate vegetation variability in northeast Africa using a molecular isotopic approach to constrain changes between plants utilizing C_3 and C_4 photosynthetic pathways. C_3 and C_4 plants exhibit distinctive stable carbon isotopic ($\delta^{13}C$) signatures (O'Leary, 1981). C_3 plants, which include nearly all trees and shrubs, have bulk leaf tissue $\delta^{13}C$ values of $-31.4‰$ to $-24.6‰$, whereas those of C_4 plants, mostly grasses adapted to water-limited or warm season precipitation conditions, fall between $-14.1‰$ and $-11.5‰$ in East Africa (Cerling et al., 1993). The range of isotopic values depends on water availability and the openness of the canopy; C_3 plants in more open or water stressed conditions display more enriched values (Cerling et al., 1997). This discrimination, associated with photosynthetic carbon fixation, is also recorded in leaf wax lipids, albeit with a systematic offset relative to bulk tissue for both plant types (O'Leary, 1981;

Table 1
Age control on β-Tulu Bor Tuff (known as Sidi Hakoma Tuff in Ethiopia)

Location	Dating technique	Dated material	Age (Ma)	Reference
Hadar, Ethiopia	$^{40}Ar/^{39}Ar$	Alkali feldspar	3.40 ± 0.03	Walter and Aronson (1993)
Wee-ee, Ethiopia	$^{40}Ar/^{39}Ar$	Alkali feldspar	3.40 ± 0.03	White et al. (1993)
Munesa, Ethiopia	$^{40}Ar/^{39}Ar$	Alkali feldspar	3.41 ± 0.01	Walter and Aronson (1993)
ODP Site 721	Orbital-tuning	Foraminifera	3.41 ± 0.01	deMenocal and Brown (1999)
Turkana Basin	Interpolation	Bracketing tuffs[a,b]	3.36 ± 0.04	Feibel et al. (1989)
Turkana Basin	Interpolation	Bracketing tuffs[a,b]	3.39 ± 0.05	Walter and Aronson (1993)
Turkana Basin	Paleomagnetism	Early Gauss Chron[b]	3.29 ± 3.57	Brown et al. (1978), Feibel et al. (1989)

[a] The β-Tulu Bor Tuff is bracketed by the radiometrically dated Toroto Tuff at 3.32 ± 0.02, stratigraphically just above the β-Tulu Bor (McDougall, 1985), and the Lokochot Tuff, located at or below the Gauss/Gilbert paleomagnetic boundary (Brown et al., 1985), indicating an age of 3.58.

[b] Age estimate corrected for the updated geomagnetic polarity timescale (Hilgen, 1991; McDougall et al., 1992).

Collister et al., 1994). Leaf waxes are readily abraded and transported by water and wind to lacustrine and marine deposits, where they are well preserved with a molecular distribution and isotopic composition that has been found to be representative of vegetation source (Meyers and Eadie, 1993; Freeman and Colarusso, 2001; Schefuss et al., 2003a). Bulk sedimentary $\delta^{13}C$ measurements are insufficient for reconstructing vegetation changes because of the multiple sources of organic carbon with different isotopic compositions delivered to both marine (Pearson and Eglinton, 2000) and lacustrine sediments (Meyers and Eadie, 1993; Meyers, 1997; Scholz et al., 2003). Molecule-specific $\delta^{13}C$ measurements of higher plant wax lipids allow carbon exclusively from terrestrial plants to be sampled (Freeman and Colarusso, 2001). Biologically-specific markers (biomarkers) diagnostic of a terrestrial higher plant leaf wax source include C_{26}–C_{32} *n*-alkanoic acids with an even/odd chain length predominance and C_{27}–C_{33} *n*-alkanes with an odd/even preference (Eglinton and Hamilton, 1967; Kolattukudy, 1969).

Vegetation reconstruction based on the carbon isotopic composition of leaf wax lipids has used *n*-alkanoic acids (Madureira et al., 1997; Simoneit, 1997; Huang et al., 1999; Conte and Weber, 2002; Eglinton et al., 2002; Hughen et al., 2004; Feakins et al., 2005), *n*-alcohols (Madureira et al., 1997; Simoneit, 1997; Huang et al., 1999; Conte and Weber, 2002; Eglinton et al., 2002; Rommerskirchen et al., 2003) and most commonly *n*-alkanes, including biomarker studies off West Africa (Simoneit, 1997; Huang et al., 1999; Huang et al., 2000; Eglinton et al., 2002; Rommerskirchen et al., 2003; Schefuss et al., 2003a; Schefuss et al., 2003b; Zhao et al., 2003; Schefuss et al., 2005). The *n*-alkanes were avoided for initial paleoecological reconstruction at DSDP Site 231 (Feakins et al., 2005) because molecular distributions, e.g. the Carbon Preference Index (CPI < 3); where $CPI = 2([C_{26}] + [C_{28}])/([C_{25}] + [C_{27}] + [C_{27}] + [C_{29}])$ indicated contamination of the plant wax signal (Feakins, unpublished data). The *n*-alkanoic acids were therefore selected because molecular distributions and carbon isotopic compositions showed that they were a reliable proxy at the site for terrestrial vegetation and abundances were generally sufficient for isotopic characterization (Feakins et al., 2005); components > C_{24} are generally thought to be derived predominantly from terrestrial plants, whereas shorter chain lengths are more likely to be influenced by microbial (algal and bacterial) contributions (Volkman et al., 1980, 1998; Canuel and Martens, 1993; Gong and Hollander, 1997; Meyers, 1997). At DSDP Site 231, C_{26}, C_{28} and C_{30} *n*-alkanoic acids have distributions diagnostic of a plant leaf wax source (CPI > 3) and exhibit carbon isotopic values within the range of modern C_3 and C_4 vegetation end members. We selected the C_{30} acid for vegetation reconstruction (Feakins et al., 2005) because it displays the largest dynamic range in isotopic values and is most likely representative of a terrestrial vegetation source (Volkman et al., 1980; Meyers, 1997; Hughen et al., 2004).

In this study we compare long chain *n*-alkane and *n*-alkanoic acid biomarkers of northeast African vegetation in lacustrine and marine depositional settings. Using the time equivalent marker horizon provided by the β-Tulu Bor Tuff, we select sediments of equivalent age and evaluate differences in molecular abundance and compound specific isotopic composition across an interval of cyclic environmental variability. We find substantial differences between compound classes and sedimentary types, complicating their interpretation in terms of paleoenvironmental reconstruction.

2. Site and sample selection

As an initial comparison of lacustrine and marine sedimentary records of leaf wax biomarkers in northeast Africa, we examine the abundance and carbon isotopic composition of long chain *n*-alkanoic acids and *n*-alkanes in sediments from DSDP Site 231 in the Gulf of Aden (11.89°N, 48.25°E) and from the Wargolo outcrop, East of Lake Turkana, Kenya (~ 3.66°N 36.25°E; Fig. 1). Samples of known time equivalence are available at both sites marked by the widespread β-Tulu Bor Tuff. We select the time period immediately prior to the β-Tulu Bor eruption, where paleogeographic reconstruction indicates that the paleolake Lokochot (~ 2500 km^2) occupied part of the Turkana Basin (Brown and Feibel, 1988; Brown and Feibel, 1991). Geomorphological reconstruction suggests that the lake formed in an open basin in response to climate, and not tectonics, as discussed in Section 1, thus presenting an ideal event for studying climate variability in the region (Brown and Feibel, 1988).

A 32 m section of the Wargolo outcrop is bracketed by the β-Tulu Bor (3.40 Ma; Table 1) and Lokochot (3.58 Ma) Tuffs (Brown et al., 1978;

McDougall et al., 1992; deMenocal and Brown, 1999) and comprises five diatomite–claystone cycles (immediately below the β-Tulu Bor Tuff) preceded by an extensive paleosol of unknown temporal duration. The 20 m thick series of alternating lacustrine claystones and diatomites suggests repeated oscillations in lake hydrology. Diatom floras are dominated by *Aulacosira*/*Melosira* cf. *M. granulate*, suggesting a shallow freshwater lake during a climatically wet period (Feibel et al., 1991). Reduced diatom abundance in clay-rich sediments is interpreted as representing an increase in salinity in the lake during relatively arid intervals. Although the diatomite–claystone cycles cannot be individually dated, we suggest that they represent precessional cyclicity given the demonstrated connection between precessional forcing and tropical climate during the Pliocene (e.g. Rossignol-Strick, 1983; Pokras and Mix, 1987; Hilgen, 1991; Tiedemann et al., 1994; deMenocal, 1995; Lourens et al., 1996; Trauth et al., 2001; Tuenter et al., 2003). In equatorial regions, where there is a bimodal annual precipitation pattern, precession-driven increases in March and September insolation occur twice in a precession cycle and have been linked to humidity increases with 10–11 ka periodicity in a record from Lake Naivasha, Kenya (Trauth et al., 2001). Unfortunately, we cannot verify whether the lacustrine depositional cycles match the number of precessional cycles in the 180 ka interval between the Lokochot and the β-Tulu Bor Tuffs, given the unknown time of paleosol formation. However diatomite sediments are likely to be associated with climatically wet periods, presumably associated with insolation forcing of stronger monsoon precipitation. We selected samples for biomarker analysis below the β-Tulu Bor Tuff at measured maxima and minima of climatic cycles as indicated by magnetic susceptibility as well as lithic (sand, silt and clay) vs. diatom abundance in the Wargolo sequence.

We selected comparable samples from the marine site, DSDP Site 231, below β-Tulu Bor Tuff, at maxima and minima of oscillations in terrigenous dust (calculated as the residual non-carbonate fracton of the sediment) in order to constrain changes in molecular abundance and isotopic composition across what have been identified as precession frequency environmental cycles (deMenocal, 1995). The sediments at the site are dated by an interpolated age model based on geochemical correlation to dated eruptions of six tephra layers in the core, including β-Tulu Bor Tuff (Sarna-Wojcicki et al., 1985; Brown et al., 1992; Feakins et al., 2007).

3. Analytical methods

Dry homogenized samples were extracted with 90% CH_2Cl_2/MeOH (9/1) using an accelerated solvent extractor. Extracts were transesterified with HCl/MeOH (5/95) at 70 °C for 12 h ($\delta^{13}C_{methanol} = -47.25‰ \pm 0.10$, $n = 3$). Excess milliQ water was added to the products and the lipids were partitioned into hexane. The hexane extracts were dried by passing them through a column of anhydrous Na_2SO_4 and separated into three fractions using column chromatography (5 cm × 4 mm Pasteur pipette, 5% water-deactivated silica gel, 100–200 mesh); alkanes were eluted with hexane and fatty acid methyl esters (FAMEs) with 5% EtAc in hexane. Urea adduction was used to remove branched and cyclic compounds from straight chain ($C \geqslant 14$) molecules (Marlowe et al., 1984). Carbon isotopic measurements were obtained using gas chromatography–isotope ratio monitoring–mass spectrometry (GC–irm–MS) with a HP6890 chromatograph, equipped with a CP Sil 5 CB column (60 m × 0.25 mm, film thickness 0.25 μm) and a Gerstel programmable injector, and interfaced via a combustion furnace at 850 °C to a Finnigan MAT Delta^{Plus} spectrometer. Samples were injected in triplicate along with reference standards of known isotopic composition. Individual transesterified *n*-alkanoic acid $\delta^{13}C$ values were corrected for derivative carbon, on the basis of isotopic mass balance.

Samples for total organic carbon (TOC) measurement were weighed into silver capsules, wetted with 10 μl ultra high purity water and placed in an evacuated desiccator oven containing an open dish of 12N HCl for 16 h. After exposure to acid, samples were dried at 60 °C, wrapped in tin capsules and compressed to ensure proper flash combustion in a Fisons Carlo Erba 1108 Elemental Analyzer.

4. Results and discussion

4.1. Biomarker abundance

Abundances are given in uncalibrated intensity units and are intended for comparison as relative values. We find large differences in abundances between samples and between marine and lacustrine depositional environments (Table 2, Figs. 2 and 3). The highest concentrations were found in the

Table 2
Molecular abundances (intensity units g dry wt^{-1}) of *n*-alkane and *n*-alkanoic acid biomarkers in lacustrine and marine sediments

Sample	Depth (mbsf)	Age (Ma)	Dust	TOC (%)	FA/Alk	*n*-Alkanes							*n*-Alkanoic acids					
						$[C_{29}]$	$[C_{31}]$	$[C_{33}]$	$[C_{31}]/[C_{29}]$	C_{max}[a]	ACL[b]	CPI[b]	$[C_{26}]$	$[C_{28}]$	$[C_{30}]$	C_{max}[a]	ACL[b]	CPI[b]
Marine samples from DSDP Site 231																		
19-2-30-45	160.80	3.400	High	1.18	0.5	66	84	50	1.3	31	29.0	2.1	30	41	22	28	27.9	4.6
19-2-75-90	161.25	3.407	High	1.40	n/a	n/a	n/a	n/a	n/a	n/a	n/a	n/a	41	50	31	28	27.9	4.5
19-2-135-150	161.85	3.414	Low	0.91	1.2	52	68	43	1.3	31	29.2	2.5	84	77	35	26	27.5	4.5
19-3-33-47	162.32	3.421	High	1.41	2.8	39	54	36	1.4	31	n/a	n/a	147	146	70	26	27.6	4.6
19-3-77-92	162.77	3.427	Low	1.29	n/a	77	114	78	1.5	31	29.7	3.4	468	n/a	208	26	n/a	n/a
19-4-0-15	163.50	3.437	High	1.13	2.8	49	69	49	1.4	31	29.6	3.7	175	190	102	28	27.7	4.5
19-4-60-75	164.10	3.445	Low	0.91	n/a	49	76	56	1.6	31	29.9	4.1	628	584	n/a	26	n/a	4.5
Mean					1.8	55	77	52	1.4	31	29.5	3.2	225	181	78	27	27.7	4.5
σ					1.2	14	20	14	0.1	0	0.4	0.8	232	206	70	1.1	0.1	0.0
Sample	Height (m)	Age (Ma)	Lith.	TOC (%)	FA/Alk	$[C_{29}]$	$[C_{31}]$	$[C_{33}]$	$[C_{31}]$ $[C_{29}]$	C_{max}	ACL	CPI	$[C_{26}]$	$[C_{28}]$	$[C_{30}]$	C_{max}	ACL	CPI
Terrestrial samples from Wargolo, Turkana Basin																		
W2340	23.4	n/a	Diatom	n/a	n/a	n/a	n/a	n/a	n/a	n/a	n/a	n/a	11	19	12	28	27.5	2.0
W2130	21.3	n/a	Clay	n/a	12.6	26	27	25.05	1.0	31	29.0	1.7	163	343	478	30	27.7	2.5
W1950	19.5	n/a	Diatom	n/a	n/a	n/a	n/a	n/a	n/a	n/a	n/a	n/a	12	27	17	28	27.6	3.2
W1800	18.0	n/a	Clay	n/a	n/a	n/a	n/a	n/a	n/a	n/a	n/a	n/a	23	43	33	28	27.6	2.0
Mean					12.6	26	27	25	1.0	31	29.0	1.7	52	108	135	29	27.6	2.4
σ					n/a	n/a	n/a	n/a	n/a	n/a	n/a	n/a	74	157	229	1	0.1	0.6
Mean – claystone only					12.6	26	27	25	1.0	31	29	1.7	93	193	256	29	27.6	2.3
σ					n/a	n/a	n/a	n/a	n/a	n/a	n/a	n/a	99	212	314	1	0.1	0.3
Mean – diatomite only					n/a	n/a	n/a	n/a	n/a	n/a	n/a	n/a	11	23	15	28	28	3
σ					n/a	n/a	n/a	n/a	n/a	n/a	n/a	n/a	1	6	3	0	0	1

[a] C_{max} = modal chain length.

[b] Standard abundance indices were calculated from concentrations using formulae: $ACL_{alkanes\,(i=25:33)} = \sum C_i * i / \sum C_i$; $ACL_{alkanoic\ acids(i=25:30)} = \sum C_i * i / \sum C_i$ and $CPI = (2 * \sum[C_n])/(\sum C_{n-1} + \sum C_{n+1})$ where $n_{n\text{-alkanoic acids}} = 26$ and 28 for and $n_{n\text{-alkanes}} = 27$, 29 and 31. FA/Alk is the ratio of abundances of *n*-alkanoic acids to *n*-alkanes: $FA/Alk = \sum[C_{29},C_{31},C_{33}]_{n\text{-alkanes}}/\sum[C_{29},C_{31},C_{33}]_{n\text{-alkanes}}$.

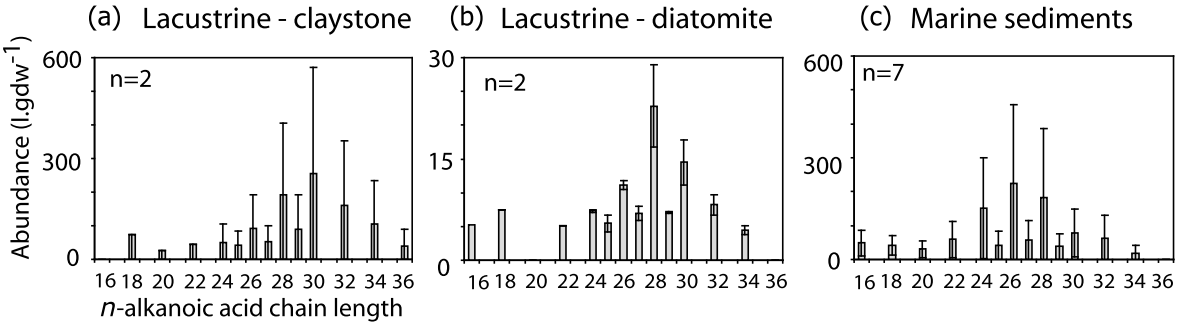

Fig. 2. Mean distributions of long chain *n*-alkanoic acids for: (a) lacustrine claystones, $n = 2$; (b) lacustrine diatomites, $n = 2$ and (c) marine sediments, $n = 7$. Abundances are reported in uncalibrated intensity units per g dry wt^{-1}; error bars denote 1σ SD between individual sample horizons in the marine core and outcrop (see Table 2). Note order of magnitude difference in *y*-axis scales.

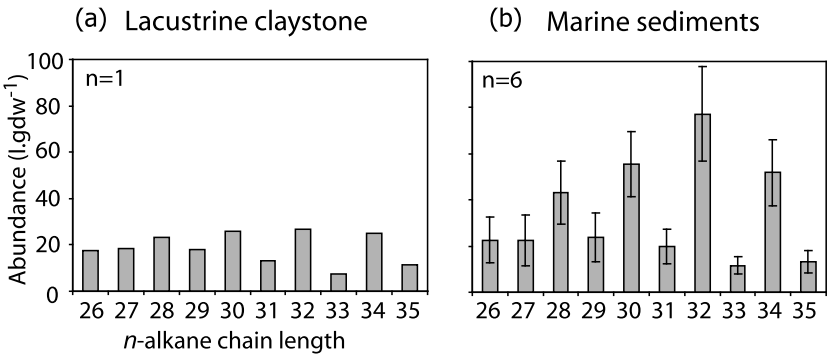

Fig. 3. Distributions of long chain *n*-alkanes for: (a) lacustrine claystone sediments, sample $n = 1$, and (b) marine sediments, $n = 6$; error bars denote 1σ SD between individual sample horizons in the marine core.

marine sediments and lacustrine claystones. The diatomaceous lacustrine sediments (samples W1950 and W2340) yielded the lowest long chain *n*-alkanoic acid abundances, with yields ca. one tenth of those in the lacustrine claystones and marine sediments (Fig. 2). Marine samples had double the abundance of *n*-alkanes compared to one lacustrine sample, a claystone (W2130, Fig. 3); *n*-alkane yields were too low to measure for the other terrestrial samples (two diatomites samples and one claystone).

Differential biomarker inputs, preservation or dilution may account for the concentration differences between sediments. Better preservation is suspected in the claystones where laminations (of the order of 1 mm thick) indicate low oxygen conditions, more degradation being expected under oxic conditions in the diatomites. In addition, if these sedimentary cycles represent equivalent length portions of the precessional cycle, with diatomaceous sediments corresponding to wet periods and claystones corresponding to drier periods, then dilution could explain the low biomarker abundance in relatively thick (higher sedimentation rate) diatom-rich deposits. In the marine sediments, fluctuations in terrigenous biomarker abundances appear to represent variations in terrigenous input to the sediments since they occur largely independent of variation in total organic carbon (TOC; Fig. 4), representing the balance of total marine and terrestrial organic inputs and diagenesis (McCaffrey et al., 1991; Madureira et al., 1997).

4.2. Ratio of n-alkanoic acid to n-alkane abundance

The *n*-alkanoic acids were found to be generally more abundant than *n*-alkanes (Table 2). In the marine sediments, summed C_{26}, C_{28} and C_{30} *n*-alkanoic acid abundances are 0.5–2.8 times more than summed C_{27}, C_{29} and C_{31} *n*-alkane abundances (FA/Alk, Table 2). In the lacustrine sediments, *n*-alkanoic acids were 12.6 times more abundant in the one claystone sample (W2130) that gave measurable concentrations of *n*-alkanes; in the

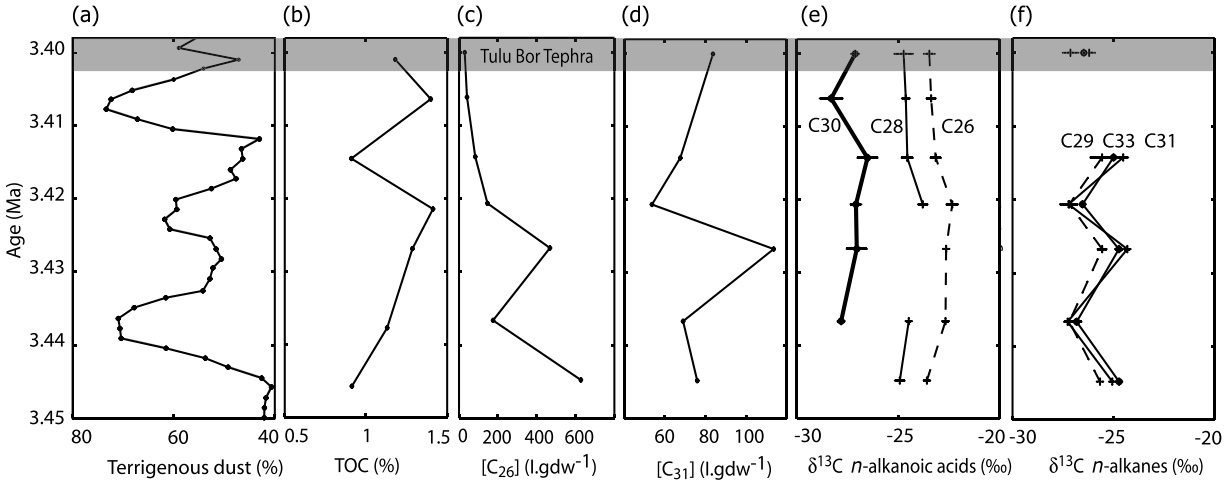

Fig. 4. Biomarker reconstructions for DSDP Site 231 showing: (a) terrigenous dust (%) calculated as the residue from $CaCO_3$ analysis (deMenocal, 1995); (b) TOC (%); (c) abundance of C_{26} *n*-alkanoic acid; (d) abundance of C_{31} *n*-alkane; (e) $\delta^{13}C$ value of selected *n*-alkanoic acids (C_{30}, C_{28} and C_{26}) and (f) $\delta^{13}C$ value of selected *n*-alkanes (C_{33}, C_{31} and C_{29}). Gray shaded bar indicates position of β-Tulu Bor Tuff.

diatomaceous sediments *n*-alkane yields were too low to be detected. The *n*-alkanoic acid to *n*-alkane ratio is therefore much higher for the terrestrial samples (at least 12.6) than the marine samples (average 1.8). The ratio of *n*-alkanoic acids/*n*-alkanes in plant leaf wax varies between species, with values between 0.5 and 2 reported for individual North American prairie species, 4 for regional aerosols (Conte et al., 2003) and 2 for marine sediments from the northwest Atlantic (Westerhausen et al., 1993; Madureira et al., 1997). The values at Site 231, between 0.5 and 2.8, are within the range measured for plants, aerosols and sedimentary deposits elsewhere. The high values in the lacustrine samples (at least 12.6) are much greater than would be expected from the composition of known plant leaf waxes and require an alternative explanation.

Diagenesis would normally be expected to reduce the abundance of the more labile *n*-alkanoic acids, decreasing the *n*-alkanoic acid/*n*-alkane ratio in ancient sediments. However a fourfold increase in the ratios has been reported for abrasion products of dead leaves vs. green leaves (Rogge et al., 1993); *n*-alkanoic acids can be produced during microbial degradation and may be ablated from decaying vegetation and remobilized soils (Conte et al., 2003), although it seems unlikely that this effect would dominate the flux of leaf wax from fresh vegetation. Very high ratio values have also been reported for conifers (Gulz, 1994), which could explain the *n*-alkanoic acid abundances in lacustrine sediments if northeast African conifers such as *Juniperus* or *Podocarpus* were present upstream of the Turkana site and accounted for almost all the leaf wax influx into the lake. *Juniperus* and *Podocarpus* are relatively common elements of highland forests in Ethiopia and Kenya today (1800–3000 m elevation, <1000 mm annual rainfall; Bonnefille, 1983; Darbyshire et al., 2003) and *Juniperus* has been documented in pollen reconstructions from Hadar, Ethiopia, between 3.4 and 2.9 Ma (Bonnefille et al., 2004). However, pollen and macrofossils dating from 3 Ma indicate tropical rainforest in the lower elevations of the Omo River (ca. 400 m elevation) close to modern Lake Turkana (Bonnefille, 1976, 1980). If there was a dense humid forest surrounding the Lokochot Lake at 3.4 Ma, it seems unlikely that coniferous *n*-alkanoic acid input from the highlands would dominate the leaf wax flux to Turkana Basin sediments.

4.2.1. A suspected microbial source of long chain n-alkanoic acids in lacustrine sediments

Since neither senescent vegetation nor plant assemblage appears to be a likely explanation for the *n*-alkanoic acid/*n*-alkane values in the lacustrine sediments, other non terrestrial plant sources must be considered. Aquatic macrophytes, algae (including diatoms) and bacteria have been shown to contribute a significant proportion of *n*-alkanoic acids and *n*-alkanes to coastal sediments (Volkman et al., 1980; Canuel and Martens, 1993; Canuel

et al., 1997). Aquatic macrophytes produce more abundant long chain *n*-alkanes than *n*-alkanoic acids (Canuel et al., 1997) and so do not seem to explain the observations here. Microbial (bacterial and algal) contributions have been shown to dwarf terrestrial plant contributions to TOC in several studies (e.g. Canuel and Martens, 1993; Gong and Hollander, 1997; Niggemann and Schubert, 2006). Although bacteria and algae may only produce small amounts of long chain *n*-alkanes and *n*-alkanoic acids, relative to shorter chain components, their contribution of long chain lipids may be significant relative to the flux from terrestrial higher plants (Volkman et al., 1980; Canuel and Martens, 1993; Gong and Hollander, 1997). We suspect that in these lacustrine sediments, particularly the diatom-rich ones, microbial sources may contribute a significant fraction of the C_{28}, and possibly other, long chain acids.

4.3. Distributions of n-alkanoic acids

Molecular abundance distribution (e.g. the CPI) gives useful information on biomarker source. Both the lacustrine and marine sediments are dominated by long chain (C_{24}–C_{32}), even *n*-alkanoic acids (Fig. 2, Table 2). CPI values of 4.5 in marine sediments point to a dominant plant wax source (Collister et al., 1994). Lower values of 2.3 for lacustrine claystones and 2.6 for diatomites are consistent with the suggestion that terrestrial plant leaf waxes are mixed with an algal or bacterial source with low CPI *n*-alkanoic acids. Thus, *n*-alkanoic acids appear to be reliable indicators of terrestrial vegetation in marine sediments, at least with respect to DSDP Site 231 (CPI 4.5), whereas the lacustrine *n*-alkanoic acid records must be treated with caution, given their relatively low CPI (< 3) and high ratio of *n*-alkanoic acids to *n*-alkanes (at least 12.6).

4.4. Molecular distributions of n-alkanes

The distributions are dominated by odd chain lengths of C_{27}–C_{33}, indicating a higher plant leaf wax source (Fig. 3). There appear to be two dominant patterns: *n*-alkanes with an odd/even preference maximizing at C_{31} (plant-derived) and an envelope of *n*-alkanes maximizing between C_{26} and C_{28}, with an unknown origin and only weak carbon preference. In the marine samples CPI values (2.1–4.1) are somewhat lower than for *n*-alkanoic acids (4.5–4.6; Table 2). The lacustrine claystone sample (W2130) with measurable *n*-alkanes has a CPI of 1.7 (vs. an *n*-alkanoic acid CPI of 2.5). Values of 1.7–4.1 indicate that *n*-alkanes have a substantial plant component but may also include variable degrees of contamination from sources with a lower CPI value.

4.4.1. Alternative sources of low CPI n-alkanes

Low CPI *n*-alkanes in the marine and lacustrine sediments could potentially be derived from petrogenic hydrocarbons or microbial sources. Petroleum is formed in active continental rift basins and has been reported both in the Turkana Basin (Morley, 1999) and in a visible bitumen horizon in Miocene age sediments from DSDP Site 231 (Cernock, 1974). However, we find no clear evidence for a petrogenic source of hydrocarbons, since *n*-alkanes occur in low or negligible concentration. Furthermore, the distribution is not diagnostic of thermal maturity: thermogenic hydrocarbons are usually characterized by a maximum $< C_{20}$ (Tissot and Welte, 1984), whereas in these Pliocene sediments there are very low abundances of *n*-alkanes $< C_{25}$. Examination for the presence of more diagnostic thermally mature biomarkers such as hopanes and steranes would provide a more definitive conclusion. It seems more likely that the long chain, low CPI *n*-alkanes in both marine and lacustrine sediments result from microbial sources (Tissot and Welte, 1984; Gong and Hollander, 1997). Algal and bacterial sources were proposed as a source of long chain alkanoic acids for the lacustrine sediments in Section 4.3. These sources, together with aquatic macrophytes (Canuel et al., 1997), could explain the low CPI *n*-alkanes in the lacustrine sample (W2130). We therefore recommend caution in interpreting terrestrial vegetation changes from long chain *n*-alkane biomarker records where low CPI values indicate contaminating sources.

4.5. Carbon isotopic compositions of n-alkanoic acids

These fall between $-28‰$ and $-22‰$ for C_{24}–C_{34} *n*-alkanoic acids in the marine samples and demonstrate a fairly consistent pattern of isotopic offsets between chain lengths (Table 3, Figs. 4 and 5). Comparison of marine sediments and lacustrine claystones demonstrates close agreement with $\delta^{13}C$ values for the C_{30} acid of between $-26‰$ and $-27‰$. This correspondence supports the choice of the C_{30} homologue for reconstructing vegetation change from the Gulf of Aden and the Cariaco

Table 3
Carbon isotopic composition of *n*-alkane and *n*-alkanoic acid biomarkers in lacustrine and marine sediments (includes offsets between biosynthetic pairs of C_{n-1}*n*-alkanes and C_n*n*-alkanoic acids)

Sample	Depth (mbsf)	Age (Ma)	Dust	TOC (%)	δ^{13}C *n*-alkanes (‰)										δ^{13}C *n*-alkanoic acids (‰)												δ^{13}C (C_{n-1} alkane − C_n alkanoic acid) (‰)				
					25	±	27	±	29	±	31	±	33	±	24	±	26	±	28	±	30	±	32	±	34	±	25–26	27–28	29–30	31–32	33–34
Marine samples from DSDP Site 231																															
19-2-30-45	160.80	3.400	High	1.18	−28.45	0.23	−26.96	0.24	−27.14	0.38	−26.21	0.29	−26.47	0.16	−24.02	0.51	−23.46	0.27	−24.73	0.46	−27.12	0.20	−24.68	0.10	−26.21	1.01	−4.99	−2.23	−0.02	−1.54	−0.26
19-2-75-90	161.25	3.407	High	1.40	n/a	n/a	n/a	n/a	n/a	n/a	n/a	n/a	n/a	n/a	−25.21	0.42	−23.38	0.23	−24.62	0.19	−28.30	0.57	−26.57	0.54	−25.99	0.23	n/a	n/a	n/a	n/a	n/a
19-2-135-150	161.85	3.414	Low	0.91	−27.58	0.56	−25.15	0.11	−25.58	0.58	−24.53	0.24	−25.01	0.26	−24.59	0.39	−23.15	0.26	−24.55	0.28	−26.51	0.50	−23.84	0.35	−26.66	0.86	−4.43	−0.60	0.94	−0.69	1.65
19-3-33-47	162.32	3.421	High	1.41	−27.29	0.44	−26.69	0.48	−27.19	0.38	−27.23	0.42	−26.54	0.06	−24.16	0.68	−22.33	0.29	−23.79	0.23	−27.08	0.27	−24.89	0.56	n/a	n/a	−4.96	−2.91	−0.11	−2.34	n/a
19-3-77-92	162.77	3.427	Low	1.29	−26.36	0.08	−24.78	0.23	−25.57	0.22	−24.33	0.15	−24.74	0.19	−23.46	0.14	−22.64	n/a	n/a	n/a	−27.04	0.50	−25.38	0.50	−25.45	0.36	−3.73	n/a	1.47	1.05	0.71
19-4-0-15	163.50	3.437	High	1.13	−27.06	0.15	−26.73	0.23	−27.19	0.25	−27.27	0.15	−26.83	0.24	−22.77	0.27	−22.67	0.16	−24.48	0.11	−27.81	0.17	−26.67	0.73	n/a	n/a	−4.39	−2.25	0.62	−0.60	n/a
19-4-60-75	164.10	3.445	Low	0.91	−26.68	0.60	−24.94	0.60	−25.67	0.02	−25.07	0.08	−24.73	0.12	−23.64	0.05	−23.58	0.15	−24.92	0.24	n/a	n/a	−24.53	0.32	n/a	n/a	−3.10	−0.01	n/a	−0.54	n/a
Mean					−27.24	0.34	−25.87	0.32	−26.39	0.31	−25.77	0.22	−25.72	0.17	−23.98	0.35	−23.03	0.23	−24.51	0.25	−27.31	0.37	−25.22	0.44	−26.08	0.61	−4.27	−1.60	0.58	−0.78	0.70
Terrestrial samples from Wargolo, Turkana Basin																															
Sample	Height (m)	Age (Ma)	Lith.	TOC (%)	25	±	27	±	29	±	31	±	33	±	24	±	26	±	28	±	30	±	32	±	34	±	25–26	27–28	29–30	31–32	33–34
W2340	23.4	n/a	Diatom	n/a	n/a	n/a	n/a	n/a	n/a	n/a	n/a	n/a	n/a	n/a	−18.88	0.19	−18.47	0.15	−18.78	0.57	−21.85	0.55	−23.54	0.52	−23.06	1.36	n/a	n/a	n/a	n/a	n/a
W2130	21.3	n/a	Clay	n/a	−28.59	0.08	−27.76	0.09	−27.74	0.30	−27.37	0.32	−26.30	0.17	−25.04	0.60	−24.83	0.49	−26.56	0.25	−26.66	0.41	−25.61	0.54	−25.25	0.19	−3.77	−1.20	−1.08	−1.76	−1.05
W1950	19.5	n/a	Diatom	n/a	n/a	n/a	n/a	n/a	n/a	n/a	n/a	n/a	n/a	n/a	−20.11	0.25	−17.07	0.74	−15.02	0.48	−18.88	0.31	−22.72	0.18	−24.50	0.69	n/a	n/a	n/a	n/a	n/a
W1800	18.0	n/a	Clay	n/a	n/a	n/a	n/a	n/a	n/a	n/a	n/a	n/a	n/a	n/a	−25.42	0.58	−25.40	0.22	−26.65	0.52	−26.84	0.18	−25.78	0.06	−25.33	0.27	n/a	n/a	n/a	n/a	n/a
Mean					−28.59	0.08	−27.76	0.09	−27.74	0.30	−27.37	0.32	−26.30	0.17	−20.11	0.25	−17.07	0.74	−15.02	0.48	−18.88	0.31	−22.72	0.18	−24.50	0.69	−3.77	−1.20	−1.08	−1.76	−1.05
Mean – claystone only					−28.59	0.08	−27.76	0.09	−27.74	0.30	−27.37	0.32	−26.30	0.17	−19.49	0.22	−17.77	0.44	−16.90	0.53	−20.37	0.43	−23.13	0.35	−23.78	1.02	−3.77	−1.20	−1.08	−1.76	−1.05
Mean – diatomite only					n/a	n/a	n/a	n/a	n/a	n/a	n/a	n/a	n/a	n/a	−25.23	0.59	−25.12	0.36	−26.60	0.39	−26.75	0.30	−25.69	0.30	−25.29	0.23	n/a	n/a	n/a	n/a	n/a

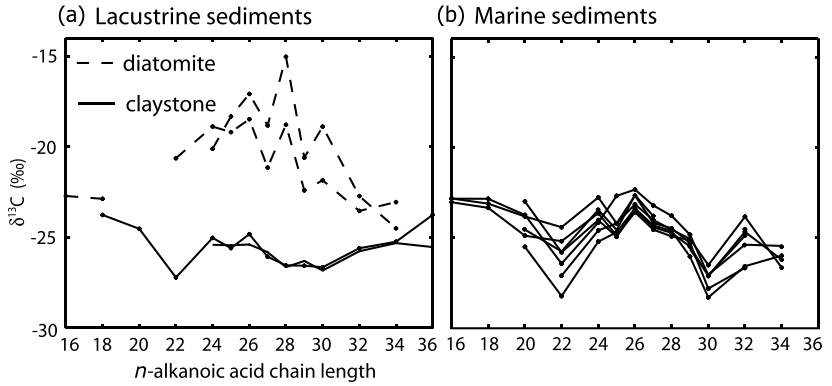

Fig. 5. The $\delta^{13}C$ value vs. chain length of *n*-alkanoic acid for: (a) lacustrine sediments – dashed line, diatomites; solid line, claystone samples and (b) marine sediments. Each line corresponds to an individual sample horizon in the marine core and outcrop.

Basin (Hughen et al., 2004; Feakins et al., 2005). The mean $\delta^{13}C$ of C_{30} (−27‰) indicates C_3 dominated vegetation type in northeast Africa in the 50 ka prior to the β-Tulu Bor eruption. Downcore reconstruction shows small amplitude variation among the six samples (< 2‰; Fig. 4e and f). Changes of 2‰ correspond to ~ 20% variability in the C_4 vegetation contribution, which is relatively small compared to the 5‰ variability on similar 10^4–10^5 year timescales observed at other times in the Plio-Pleistocene at Site 231 (Feakins et al., 2005). In contrast, there are large isotopic offsets between *n*-alkanoic acids in the Turkana Basin diatomite and claystone samples, as well as distinct patterns of isotopic composition as a function of chain length (Figs. 5a, 7 and 8). Values are up to 10‰ more enriched for C_{24}–C_{34} *n*-alkanoic acids from the diatomaceous sediments (−24‰ to −15‰) relative to the claystone samples (−27‰ to −24‰; Fig. 5a), resulting in very different downcore reconstructions depending on the choice of homolog (Fig. 7). The value for C_{30} varies between −27‰ (claystone) and −18.6‰ (diatomite), beyond the range for the marine samples from Site 231 (−30‰ to −22‰; Feakins et al., 2005), and exceeding the range for modern plant leaf waxes.

C_4 plants have been measured with bulk $\delta^{13}C$ compositions between −9‰ and −15‰ (Cerling et al., 1997), with a relative depletion for *n*-alkanes of < 10‰ (Collister et al., 1994) and a smaller depletion for *n*-alkanoic acids, suggesting an approximate range of −19‰ to −25‰ for the leaf wax *n*-alkanes and *n*-alkanoic acids of C_4 plants. The most common C_4 grass near the modern lake and on dry stream beds is *Sporobolus spicatus* (F.H. Brown, personal communication), a C_4 halophyte with bulk tissue $\delta^{13}C$ value of −13‰ (Schulze et al., 1996). An increase in C_4 species growing along the lake margin, such as *S. spicatus*, *Cyperus papyrus* or *C. latifolius*, could produce an isotopic enrichment in the sedimentary

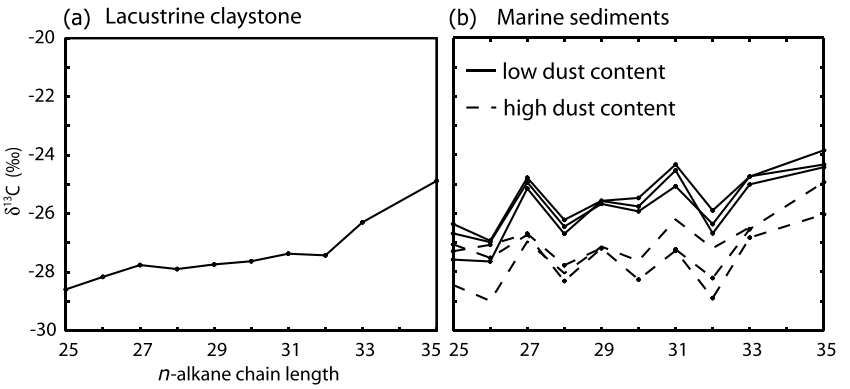

Fig. 6. The $\delta^{13}C$ value vs. chain length of *n*-alkane for: (a) a terrestrial claystone (W2130) and (b) marine samples from DSDP Site 231, solid line samples with low terrigenous dust content (< 60%), dashed line samples with high terrigenous dust content (> 60%).

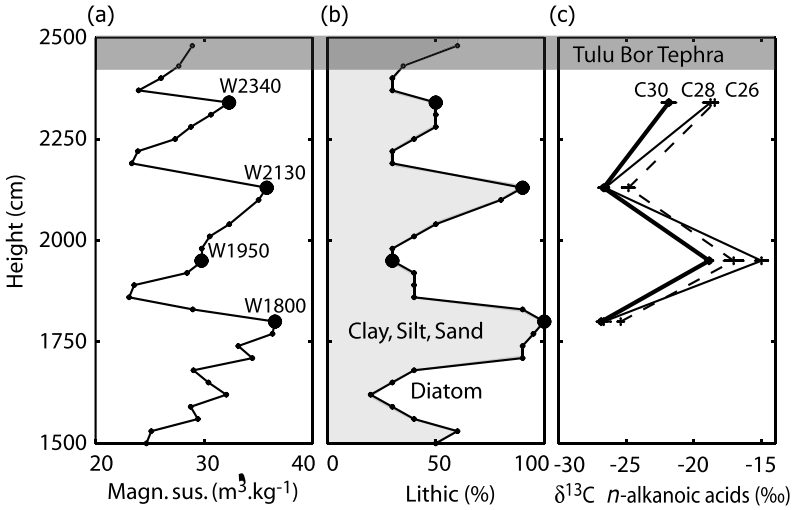

Fig. 7. Stratigraphy of Wargolo, East of Lake Turkana, Kenya: (a) magnetic susceptibility; (b) relative abundance of lithic grains (sum of clay, sand and silt%) vs. diatom abundance, determined by semi-quantitative smear slide counts and (c) biomarker reconstructions showing $\delta^{13}C$ value of selected *n*-alkanoic acids (C_{30}, C_{28} and C_{26}). N.B. the *n*-alkane yields were too low to measure for all samples except W2130 with the highest biomarker abundance; *n*-alkane $\delta^{13}C$ values for W2130 (not shown) are within 1‰ of the *n*-alkanoic acid values. Gray shaded bar indicates position of β-Tulu Bor Tuff.

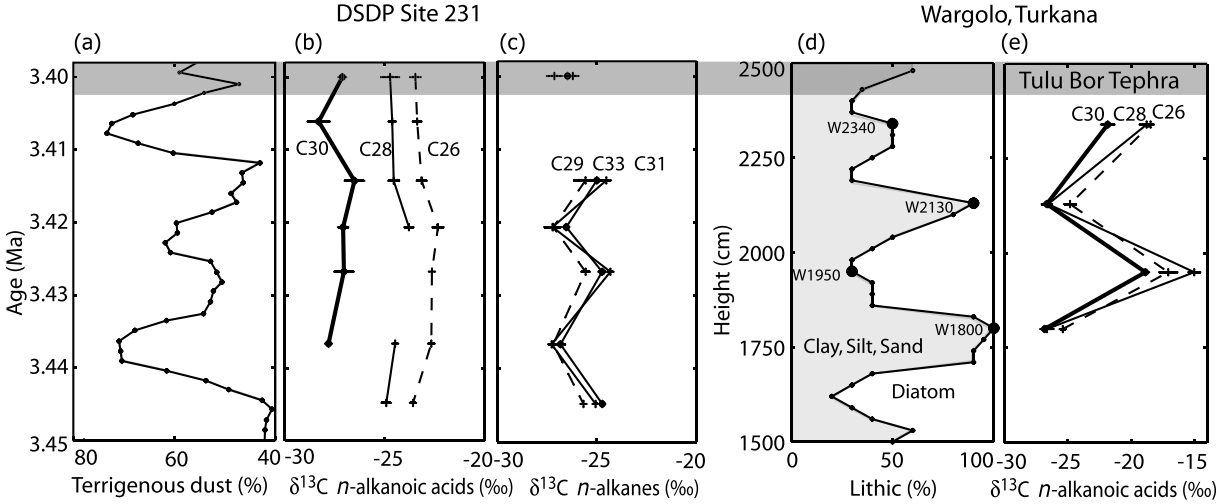

Fig. 8. Comparison of environmental reconstructions based on position of β-Tulu Bor Tuff (gray bar) showing: (a) terrigenous dust (deMenocal, 1995); (b) $\delta^{13}C$ value of selected *n*-alkanoic acids (C_{30}, C_{28} and C_{26}) and (c) $\delta^{13}C$ value of selected *n*-alkanes (C_{33}, C_{31} and C_{29}) for DSDP Site 231 and (d) lithic abundance (clay, sand, silt%) and (e) $\delta^{13}C$ value of selected *n*-alkanoic acids (C_{34}, C_{32} and C_{30}) for Wargolo, East of Lake Turkana, Kenya.

biomarkers, but we can find no explanation for an increase in C_4 vegetation associated with diatomaceous lake phases. Furthermore, even a dramatic increase in C_4 plant inputs (such as *S. spicatus* with an expected value of $\sim -23‰$ for leaf wax lipids) does not appear to be sufficient to explain values as enriched as $-18.6‰$ and $-15‰$ for C_{30} and C_{28} *n*-alkanoic acids, respectively (Fig. 5). A second problem with interpreting the isotopic shift as a C_4 expansion is the distinct pattern of isotopic composition vs. chain length in the diatomaceous and claystone samples (Fig. 5). We observe a strong trend of decreasing $\delta^{13}C$ value between the C_{28}, C_{30} and C_{32} *n*-alkanoic acids in the diatomaceous sediments, not seen in the claystone samples. Longer chain homologues are expected to be depleted in ^{13}C because kinetic isotope

fractionation effects allow fatty acids with the ^{13}C depleted carboxyl group in the acetate building blocks to be more rapidly incorporated into complex lipids during chain elongation (Monson and Hayes, 1978). Inter-species differences in kinetic isotope effects are expected (DeNiro and Epstein, 1977) and may explain observed differences in the patterns of carbon isotopic composition within a homologous series (Rieley et al., 1993; Collister et al., 1994; Boom et al., 2002; Nguyen Tu et al., 2004). However, we note that, for the marine samples at least, the pattern is highly consistent and isotopic minima for the C_{22} and C_{30} *n*-alkanoic acids are robust features of all samples from the marine site (Fig. 5). It remains possible, but unlikely, that an increase in C_4 vegetation could account for the isotopic enrichment and steepened trend in depletion with increasing chain length in the diatomite sample compared to the claystone or marine samples. Alternatively, changing isotopic offsets could indicate aquatic sources of long chain *n*-alkanoic acids during the different sedimentation conditions in the lake. A change in biomarker source might be attributed to drastically different lake ecology and productivity that resulted in shifts between claystone and diatomite sedimentation. While algae produce abundant *n*-alkanoic acids in the range C_{14}–C_{20}, they also produce longer chain fatty acids (C_{20}–C_{30}), typically only $< 5\%$ of the C_{14}–C_{20} production, but since these longer chain lengths are more refractory they may be better represented in the sedimentary record (Volkman et al., 1980, 1998; Canuel and Martens, 1993). In one study, diatoms (including *Aulacosira*/*Melosira*) have been suggested to contribute 30–80% of C_{24} to C_{28} *n*-alkanoic acids (Volkman et al., 1980). In other studies silica-bound lipids have been documented in diatoms in sediments of glacial age (Crosta and Shemesh, 2002; Crosta et al., 2002). Isotopic compositions of biomarkers (C_{23} and C_{25} *n*-alkanes and isoprenoid alkenes) for lacustrine algae in East Africa have been measured in the range of $-35‰$ to $-12.5‰$ (Street-Perrott et al., 2004). Under stratified or hypersaline conditions, CO_2 drawdown can occur, producing enriched $\delta^{13}C$ values in algal blooms (Laws et al., 1995); values as close to zero as $-5‰$ have been reported for some algal alkenes (Huang et al., 1999). Diatoms and other algae are therefore a potential source of the enriched isotopic values (up to $-15‰$) observed for certain *n*-alkanoic acid homologues (especially C_{26}, C_{28} and C_{30}) in the diatomite samples from the Wargolo outcrop (Fig. 5).

Bacteria are another potential source of long chain fatty acids. In a study of Santa Monica Basin, off the Californian Margin, they were found to be an important contributor of long chain fatty acids (Gong and Hollander, 1997). While they dominantly produce short chain fatty acids, they may also produce smaller amounts of long chain acids. Bacterial contamination of the higher plant signal may be significant where bacterial populations rise, with up to 50% of TOC attributed to bacterial sources in some sediments (Alongi, 1988). However, the carbon isotopic values of *n*-alkanoic acids from bacteria are typically lower than would be expected for terrestrial plants (Gong and Hollander, 1997) and therefore algae appear to be the more likely source here. Most algae produce low abundances of *n*-alkanes (Volkman et al., 1980) which may also explain the high *n*-alkanoic acid/*n*-alkane ratio in lacustrine sediments (Table 2). Thus, comparing the *n*-alkanoic and alkane data for the same samples may yield insights into terrestrial higher plant vs. microbial sources of long chain *n*-alkyl lipids. Unfortunately, we were unable to measure *n*-alkane $\delta^{13}C$ values for most of the lacustrine sediments because of the low concentrations. We therefore recommend cautious interpretation of the lacustrine *n*-alkanoic acid isotopic record, which may include a significant microbial component, most likely derived from *Aulacosira*/*Melosira* diatoms, whose tests are clearly represented in the sedimentary record (Fig. 7).

4.6. n-Alkane carbon isotopic distribution

Carbon isotopic compositions range between $-29‰$ and $-24‰$ for C_{25}–C_{33} *n*-alkanes in the marine samples (Table 3, Fig. 6b). Offsets between C_{29}, C_{31} and C_{33} *n*-alkanes are $< 1‰$ for the marine samples, much smaller than the $5‰$ spread between the C_{30}, C_{28} and C_{26} *n*-alkanoic acids (Fig. 8). Only one terrestrial sample had a sufficient abundance of *n*-alkanes for isotopic analysis, W2130 (a claystone), with values between $-29‰$ and $-2‰$ (Table 3, Fig. 6a).

The *n*-alkane and *n*-alkanoic acid isotopic compositions are not entirely consistent with an identical higher plant source. Kinetic isotope effects in the enzymatic decarboxylation of an *n*-alkanoic acid to produce an *n*-alkane should result in a small ($\sim 1‰$) depletion for the C_{n-1} *n*-alkane product relative to its C_n *n*-alkanoic acid source (O'Leary, 1976). However, we find unexpectedly large offsets ($> 3‰$) and relatively enriched *n*-alkanes (Table 3). In the one terrestrial claystone the pattern of offsets

suggests that the longer chain lengths ($> C_{26}$) are more reliably derived from higher plants (Table 3). The differences in isotopic composition suggest that carbon isotopic reconstructions may also differ between the terrestrial and marine sites depending on the type of compound (*n*-alkanoic acid or *n*-alkane) and choice of homolog.

The marine samples show offsets of up to 2‰ between odd *n*-alkanes and adjacent even *n*-alkanes, a pattern much less pronounced for the terrestrial sample (Fig. 6). Multiple sources of *n*-alkanes in marine sediments may explain the isotopic offset between even and odd chain lengths as well as the low CPI values for certain samples (Table 3, Fig. 3; Pearson and Eglinton, 2000). The *n*-alkanes in the Gulf of Aden sediments may include high CPI *n*-alkanes from plant waxes and low CPI *n*-alkanes from microbial or petrogenic sources. Mixing of high CPI plant waxes and microbial or petrogenic hydrocarbons (CPI $\sim$ 1) would result in odd chain length *n*-alkanes being dominated by the plant wax component, and even chain lengths more heavily influenced by the low CPI *n*-alkanes (Reddy et al., 2000). A mixing model correction can be applied to ''remove'' contamination of isotopic values for odd chain *n*-alkanes in sediments with low CPI values (Huang et al., 2000), although the trend of decreasing CPI in the 6 samples of decreasing age below the β-Tulu Bor (Table 2) cannot explain the pattern of variability seen downcore (Fig. 4). The C_{29} *n*-alkane is biosynthetically related to the C_{30} *n*-alkanoic acid in plant leaf wax biosynthesis and is therefore of interest for comparison, although we note that the C_{29}–C_{33} homologues display almost identical isotopic shift (Fig. 4). The marine sediments display 3‰ variability downcore (Fig. 4), slightly greater than the 2‰ for the *n*-alkanoic acids (Fig. 8), although the low CPI values make the *n*-alkane result less reliable. The $\delta^{13}C$ value for the one lacustrine claystone sample (W2130) indicates dominantly C_3 vegetation, consistent with pollen evidence for moist forest taxa in the Turkana Basin ca. 3 Ma (Bonnefille and Letouzey, 1976). However, the low CPI value (1.7) for this sample indicates that the *n*-alkanes are unlikely to be exclusively derived from higher plants.

4.7. Biomarker interpretation for vegetation reconstruction

Carbon isotopic values suggest a modest increase in the openness or water-stress of C_3 vegetation or an increase in the proportion of C_4 vegetation (normally associated with aridity) at times of low terrigenous dust input (< 60%) during this interval of the Pliocene 3.40–3.45 Ma (Figs. 4 and 8). This is somewhat surprising since low dust flux has been correlated with humid source conditions during the Pleistocene (e.g. Clemens and Prell, 1990; Tiedemann et al., 1994; deMenocal, 1995; deMenocal et al., 2000). However, deMenocal (1995) observed that the precessional dust maxima covaried in phase with summer monsoonal upwelling indices at Arabian Sea Ocean Drilling Program (ODP) Site 721/722 between 5.1 and 6.3 Ma. Prior to the onset of northern hemisphere glaciation (ca. 2.8 Ma) monsoon maxima (and dust flux increase associated with stronger transport capability) appear to respond directly to boreal summer insolation forcing (deMenocal and Bloemendal, 1995; deMenocal, 1995; Clemens et al., 1996). This pattern is consistent with modern seasonal observations that indicate increased dust flux associated with the seasonal increase in transport capacity associated with the summer southwest monsoon (Clemens, 1998). These studies therefore suggest that Pliocene dust maxima record periods of enhanced monsoon intensity, with stronger summer monsoonal winds transporting more mineral dust. Following this interpretation the DSDP Site 231 record suggests that C_3 vegetation increases in northeast Africa during monsoon maxima between 3.40 and 3.45 Ma, indicated by increased dust and organic carbon flux for the same samples. C_4 vegetation apparently increased during arid monsoon minima.

Although the β-Tulu Bor Tuff provides an excellent means of regional correlation, we have been unable to directly compare the terrestrial and marine records of vegetation, given the suspected microbial contamination of long chain *n*-alkanoic acid biomarkers in the lacustrine sediments. Terrestrial sediments reveal shifts in *n*-alkanoic acid $\delta^{13}C$ values between claystone and diatomite strata of between 2‰ and 10‰ depending on choice of homolog (Fig. 8). Enriched isotopic values during wet intervals (diatomites) appear to be caused by diatom production of long chain *n*-alkanoic acids and likely CO_2 drawdown during the diatom bloom. One sample yielding *n*-alkanes does indicate C_3 vegetation around paleolake Lokochot ca. 3.4 Ma. Although we cannot securely interpret the Wargolo biomarker record in terms of vegetation at present, these initial data suggest that precessionally paced environmental changes in the Turkana Basin were

even more pronounced than the regional vegetation changes recorded in the marine sedimentary record.

4.8. Environmental variability and hominin evolution

While it may be more difficult to generate vegetation biomarker records from terrestrial outcrops rather than marine sediments, there remains considerable motivation given the application of such records to reconstructing local environments associated with hominin fossil sites in northeast Africa, particularly given the poor preservation of pollen in many arid environments. We attempted to compare terrestrial and marine sedimentary archives of plant leaf wax biomarkers below the β-Tulu Bor Tuff, a widespread regional stratigraphic marker. This time period is of interest because the Lokochot and β-Tulu Bor Tuffs bracket the KNM-WT 40000 cranium in the Nachukui Formation, part of the Turkana Basin, Kenya (Fig. 1), attributed to *Kenyanthropus platyops* (Leakey et al., 2001). Hominins probably used lake margin environments in the Turkana Basin (Leakey et al., 2001) and would have experienced the cyclic variations in lake deposits between 3.45 and 3.40 Ma documented here. During this interval wind blown dust concentration at DSDP Site 231 varies by over 30% (deMenocal and Bloemendal, 1995) and the carbon isotopic composition of plant wax biomarkers records 2–3‰ variability, interpreted as shifts in the openness or water-stress of C_3 vegetation or variability in the proportion of C_4 grassland cover in northeast Africa (Feakins et al., 2005). This comparison of marine and terrestrial archives indicates that there may have been significant environmental variability between the Lokochot and β-Tulu Bor Tuffs corresponding to the time interval when *K. platyops* occupied the Turkana Basin.

5. Conclusions

The β-Tulu Bor Tuff provides a well dated, widely dispersed, and time equivalent marker horizon with which to compare biomarker records of northeast African vegetation in both marine and lacustrine sediments. In the marine sediments from DSDP Site 231, we observe downcore $\delta^{13}C$ variations of 2‰ in individual *n*-alkanoic acids, during the interval 3.40–3.45 Ma, which may indicate shifts in the openness or water-stress of C_3 vegetation or up to 20% variation in the proportion of C_4 vegetation cover. The *n*-alkanes indicate a slightly greater variability (up to 3‰), although the low CPI values suggest possible microbial reworking. Biomarker reconstructions for DSDP Site 231 therefore indicate significant vegetation change in the 50–100 ka prior to the β-Tulu Bor eruption, likely modulated by precessional variation in insolation. Isotopic shifts at the terrestrial site may be contemporary with shifts in the marine sediments although there is only one chronological tie point at 3.40 Ma at the terrestrial site; *n*-alkanoic acid shifts of up to 10‰ between claystone and diatomite strata in the lacustrine sediments may indicate large amplitude vegetation changes in the catchment. However, it appears more likely that diatoms are a significant source of isotopically enriched values for certain *n*-alkanoic acid homologs in the diatomaceous sediments. These initial data suggest that lacustrine sediments would likely record large amplitude changes in local vegetation if plant derived biomarkers could be disentangled from the suspected microbial contribution.

Acknowledgements

We are grateful to Frank Brown for many helpful discussions and for assistance in the field together with Ian McDougall, Craig Feibel who proposed the initial idea for comparing the terrestrial and marine biomarker records near the β-Tulu Bor, Sunny Hwang, Daniel Montluçon and Carl Johnson who helped with laboratory analysis and for the helpful contributions of two anonymous reviewers. Funding was provided by the US National Science Foundation HOMINID Grant 0218511. This is Lamont-Doherty Earth Observatory Publication Number 6994.

Associate Editor—**E.A. Canuel**

References

Alongi, D.M., 1988. Bacterial productivity and microbial biomass in tropical mangrove sediments. Microbial Ecology 15, 59–79.

Bonnefille, R., 1976. Palynological evidence for an important change in the vegetation of the Omo Basin between 2.5 and 2 million years. In: Coppens, Y., Howell, F.C., Isaa, G., Leakey, R. (Eds.), Earliest Man and Environments in the Lake Rudolf Basin. University of Chicago Press, Chicago, pp. 421–423.

Bonnefille, R., 1980. Vegetation history of savanna in East Africa during the Plio-Pleistocene. In: Proceedings of the IV International Palynological Conference, Lucknow, vol. 3, pp. 75–89.

Bonnefille, R., 1983. Evidence for a cooler and drier climate in the Ethiopian uplands towards 2.5 Myr ago. Nature 303, 487–491.

Bonnefille, R., Letouzey, R., 1976. Fruits fossiles d'Antrocaryon dans la vallee de l'Omo (Ethiopie). Adansonia 16, 65–82.

Bonnefille, R., Potts, R., Chalie, F., Jolly, D., Peyron, O., 2004. High-resolution vegetation and climate change associated with Pliocene *Australopithecus afarensis*. Proceedings of the National Academy of Sciences of the USA 101, 12125–12129.

Boom, A., Marchant, R., Hooghiemstra, H., Sinnighe Damsté, J.S., 2002. CO_2- and temperature-controlled altitudinal shifts of C_4- and C_3-dominated grasslands allow reconstruction of palaeoatmospheric pCO_2. Palaeogeography Palaeoclimatology Palaeoecology 177, 151–168.

Brown, F.H., 1982. Tulu Bor tuff at Koobi Fora correlated with Sidi Hakoma tuff at Hadar. Nature 300, 631–635.

Brown, F., Feibel, C., 1988. "Robust" hominids and Plio-Pleistocene paleogeography of the Turkana Basin, Kenya and Ethiopia. In: Grine, F. (Ed.), Evolutionary History of the "Robust" *Australopithecines*. Aldine de Gruyter, New York, pp. 325–340.

Brown, F.H., Feibel, C.S., 1991. Stratigraphy, depositional environments and palaeogeography of the Koobi Fora Formation. In: Harris, J.M. (Ed.), The Fossil Ungulates: Geology, Fossil Artiodactyls, and Palaeoenvironments, vol. 3. Clarendon Press, Oxford, pp. 1–30.

Brown, F., McDougall, I., Davis, T., Maier, R., 1985. An integrated Plio-Pleistocene chronology of the Turkana Basin. In: Delson, E. (Ed.), Paleoanthropology: The Hard Evidence. Alan R Liss, New York, pp. 82–90.

Brown, F., Shuey, R., Croes, M., 1978. Magnetostratigraphy of the Shungura and Usno Formations southwestern Ethiopia: new data and comprehensive reanalysis. Geophysical Journal of the Royal Astronomical Society 54, 519–538.

Brown, F.H., Sarna-Wojcicki, A.M., Meyer, C.E., Haileab, B., 1992. Correlation of Pliocene and Pleistocene tephra layers between the Turkana Basin of East Africa and the Gulf of Aden. Quaternary International 13–14, 55–67.

Canuel, E.A., Martens, C.S., 1993. Seasonal variations in the sources and alteration of organic-matter associated with recently-deposited sediments. Organic Geochemistry 20, 563–577.

Canuel, E.A., Freeman, K.H., Wakeham, S.G., 1997. Isotopic compositions of lipid biomarker compounds in estuarine plants and surface sediments. Limnology and Oceanography 42, 1570–1583.

Cerling, T.E., Harris, J.M., MacFadden, B.J., Leakey, M.G., Quade, J., Eisenmann, V., Ehleringer, J.R., 1997. Global vegetation change through the Miocene/Pliocene boundary. Nature 389, 153–158.

Cerling, T.E., Wang, Y., Quade, J., 1993. Expansion of C_4 ecosystems as an indicator of global ecological change in the late Miocene. Nature 361, 344–345.

Cernock, P., 1974. Geochemical analyses of potential petroleum source beds. Initial Reports of the Deep Sea Drilling Project 24, 791–797.

Clemens, S.C., 1998. Dust response to seasonal atmospheric forcing: proxy evaluation and calibration. Palaeoceanography 13, 471–490.

Clemens, S.C., Prell, W.L., 1990. Late Pleistocene variability of Arabian Sea summer monsoon winds and continental aridity: eolian records from the lithogenic component of deep-sea sediments. Paleoceanography 5, 109–145.

Clemens, S.C., Murray, D.W., Prell, W.L., 1996. Nonstationary phase of the Plio-Pleistocene Asian monsoon. Science 274, 943–948.

Cohen, A., Lezzar, K.E., Tiercelin, J.J., Soreghan, M., 1997. New palaeogeographic and lake-level reconstructions of Lake Tanganyika: implications for tectonic, climatic and biological evolution in a rift lake. Basin Research 9, 107–132.

Collister, J., Rieley, G., Stern, B., Eglinton, G., Fry, B., 1994. Compound-specific $\delta^{13}C$ analyses of leaf lipids from plants with differing carbon dioxide metabolisms. Organic Geochemistry 21, 619–627.

Conte, M., Weber, J., 2002. Plant biomarkers in aerosols record isotopic discrimination of terrestrial photosynthesis. Nature 417, 639–641.

Conte, M., Weber, J., Carlson, P., Flanagan, L., 2003. Molecular and carbon isotopic composition of leaf wax in vegetation and aerosols in a northern prairie ecosystem. Oecologia 135, 67–77.

Crosta, X., Shemesh, A., 2002. Reconciling down-core anti-correlation of diatom carbon and nitrogen isotopic ratios from the Southern Ocean. Paleoceanography 17, 1010. doi:10.1029/2000PA00056.

Crosta, X., Shemesh, A., Salvignac, M.E., Gildor, H., Yam, R., 2002. Late Quaternary variations of elemental ratios (C/Si and N/Si) in diatom-bound organic matter from the Southern Ocean. Deep Sea Research 49, 1939–1952.

Darbyshire, I., Lamb, H., Umer, M., 2003. Forest clearance and regrowth in northern Ethiopia during the last 3000 years. Holocene 13, 537–546.

de Heinzelin, J., 1983. The Omo group: archives of the International Omo Research Expedition. In: de Heinzelin, J. (Ed.), The Omo Group: Archives of the International Research Expedition. Musee Royal de L'Afrique Centrale, Tervuren.

deMenocal, P., Bloemendal, J., 1995. Plio-Pleistocene climatic variability in subtropical Africa and the paleoenvironment of hominid evolution: a combined data-model approach. In: Vrba, E., Denton, G., Partridge, T., Burckle, L. (Eds.), Paleoclimate and Evolution. Yale University Press, New Haven, pp. 262–288.

deMenocal, P.B., 1995. Plio-Pleistocene African climate. Science 270, 53–59.

deMenocal, P.B., 2004. African climate change and faunal evolution during the Pliocene-Pleistocene. Earth and Planetary Science Letters 220, 3–24.

deMenocal, P.B., Brown, F.H., 1999. Pliocene tephra correlations between East African hominid localities, the Gulf of Aden, and the Arabian Sea. In: Agusti, J., Rook, L., Andrews, P. (Eds.), Hominid Evolution and Climatic Change in Europe, vol. 1. Cambridge University Press, pp. 23–54.

deMenocal, P.B., Ortiz, J., Guilderson, T., Adkins, J., Sarnthein, M., Baker, L., Yarusinsky, M., 2000. Abrupt onset and termination of the African Humid Period: rapid climate responses to gradual insolation forcing. Quaternary Science Reviews 19, 347–361.

DeNiro, M.J., Epstein, S., 1977. Mechanism of carbon isotope fractionation associated with lipid synthesis. Science 197, 261–263.

Eglinton, G., Hamilton, R., 1967. Leaf epicuticular waxes. Science 156, 1322.

Eglinton, T., Eglinton, G., Dupont, L., Sholkovitz, E., Montlucon, D., Reddy, C., 2002. Composition, age and provenance of organic matter in NW African dust over the Atlantic Ocean. Geochemistry Geophysics Geosystems 3, 1–27.

Feakins, S.J., deMenocal, P.B., Eglinton, T.I., 2005. Biomarker records of Late Neogene changes in East African vegetation. Geology 33, 977–980.

Feakins, S., Brown, F., de Menocal, P., 2007. Plio-Pleistocene Microtephra in DSDP Site 231, Gulf of Aden. Journal of African Earth Sciences, doi:10.1016/j.jafrearsci.2007.05.004.

Feibel, C.S., 1997. A terrestrial auxiliary stratotype point and section for the Plio-Pleistocene boundary in the Turkana Basin, East Africa. Quaternary International 40, 73–79.

Feibel, C.S., 1999. Basin evolution, sedimentary dynamics and hominid habitats in East Africa: an ecosystem approach. In: Bromage, T., Schrenk, F. (Eds.), African Biogeography, Climate Change, and Human Evolution. Oxford University Press, Oxford, pp. 276–281.

Feibel, C., 2003. Stratigraphy and depositional history of the Lothagam Sequence. In: Leakey, M., Harris, J. (Eds.), Lothagam: The Dawn of Humanity in Eastern Africa. Columbia University Press, New York, pp. 17–29.

Feibel, C., Brown, F., McDougal, I., 1989. Stratigraphic context of fossil hominids from the Omo Group deposits, northern Turkana Basin, Kenya and Ethiopia. American Journal of Physical Anthropology 78, 595–622.

Feibel, C.S., Harris, J.M., Brown, F.H., 1991. Paleoenvironmental context for the late Neogene of the Turkana Basin. In: Harris, J.M. (Ed.), The Fossil Ungulates: Geology, Fossil Artiodactyls, and Palaeoenvironments, vol. 3. Clarendon Press, Oxford, pp. 321–370.

Freeman, K., Colarusso, L., 2001. Molecular and isotopic records of C_4 grassland expansion in the late Miocene. Geochimica et Cosmochimica Acta 65, 1439–1454.

Gong, C., Hollander, D., 1997. Differential contribution of bacteria to sedimentary organic matter in oxic and anoxic environments, Santa Monica Basin, California. Organic Geochemistry 26, 545–563.

Gulz, P., 1994. Epicuticular leaf waxes in the evolution of the plant kingdom. Journal of Plant Physiology 143, 453–464.

Hilgen, F.J., 1991. Astronomical calibration of Gauss to Matuyama sapropels in the Mediterranean and implication for the geomagnetic polarity time scale. Earth and Planetary Science Letters 104, 226–244.

Huang, Y., Street-Perrot, F.A., Perrott, R.A., Metzger, P., Eglinton, G., 1999. Glacial-interglacial environmental changes inferred from molecular and compound-specific $\delta^{13}C$ analyses of sediments from Sacred Lake, Mt. Kenya. Geochimica et Cosmochimica Acta 63, 1383–1404.

Huang, Y.S., Dupont, L., Sarnthein, M., Hayes, J.M., Eglinton, G., 2000. Mapping of C_4 plant input from North West Africa into North East Atlantic sediments. Geochimica et Cosmochimica Acta 64, 3505–3513.

Hughen, K., Eglinton, T., Xu, L., Makou, M., 2004. Abrupt tropical vegetation response to rapid climate changes. Science 304, 1955–1959.

Johnson, T., Brown, E., McManus, J., Barry, S., Barker, P., Gasse, F., 2002. A high-resolution paleoclimate record spanning the past 25,000 years in Southern East Africa. Science 296, 114–116.

Kalnay, E., Kanamitsu, M., Kistler, R., Collins, W., Deaven, D., Gandin, L., Iredell, M., Saha, S., White, G., Woolen, J., Zhu, Y., Chelliah, M., Ebisuzaki, W., Higgins, W., Janowiak, J., Mo, K., Ropelewski, C., Wang, J., Leetma, A., Reynolds, R., Jenne, R., Joseph, D., 1996. The NCEP/NCAR 40 year reanalysis project. Bulletin of the American Meteorological Society 77, 437–471.

Kolattukudy, P., 1969. Plant waxes. Lipids 5, 259–275.

Laws, E.A., Popp, B.N., Bidigare, R.R., Kennicutt, M.C., Macko, S.A., 1995. Dependence of phytoplankton carbon isotopic composition on growth-rate and $[CO_2]_{(aq)}$ – theoretical considerations and experimental results. Geochimica et Cosmochimica Acta 59, 1131–1138.

Leakey, M.G., Spoor, F., Brown, F.H., Gathogo, P.N., Klarie, C., Leakey, L.N., McDougall, I., 2001. New hominin genus from eastern Africa shows diverse middle Pliocene lineages. Nature 410, 433–440.

Lezine, A.-M., 1991. Correlated oceanic and continental records demonstrate past climate and hydrology of North Africa. Geology 19, 307–310.

Lourens, L.J., Antonarakou, A., Hilgen, F., Van Hoof, A.A.M., Vergnaud-Grazzini, C., Zachariasse, W.J., 1996. Evaluation of the Plio-Pleistocene astronomical timescale. Paleoceanography 11, 391–413.

Madureira, L., van Kreveld, S., Eglinton, G., Conte, M., Ganssen, G., van Hinte, J., Ottens, J., 1997. Late Quaternary high-resolution biomarker and other sedimenary climate proxies in a northeast Atlantic core. Paleoceanography 12, 255–269.

Marlowe, I., Brassell, S.C., Eglinton, G., Green, J., 1984. Long chain unsaturated ketones and esters in living algae and marine sediments. Organic Geochemistry 6, 135–141.

McCaffrey, M., Farrington, J., Repeta, D., 1991. The organic geochemistry of Peru margin surface sediments: II. Paleoenvironmental implications of hydrocarbon and alcohol profiles. Geochimica et Cosmochimica Acta 55, 483–498.

McDougall, I., 1985. $^{40}Ar/^{39}Ar$ dating of the hominid bearing Plio-Pleistocene sequence at Koobi-Fora, Lake Turkana, northern Kenya. Bulletin of the Geological Society of America 96, 159–175.

McDougall, I., Brown, F.H., Cerling, T.E., Hillhouse, J.W., 1992. A reappraisal of the geomagnetic polarity time scale to 4 Ma using data from the Turkana Basin, East-Africa. Geophysical Research Letters 19, 2349–2352.

Meyers, P., 1997. Organic geochemical proxies of paleoceanographic, paleolimnologic, and paleoclimatic processes. Organic Geochemistry 27, 213–250.

Meyers, P., Eadie, B., 1993. Sources, degradation, and recycling of organic matter associated with sinking particles in Lake Michigan. Organic Geochemistry 20, 47–56.

Monson, K., Hayes, J.M., 1978. Carbon isotopic fractionation in the biosynthesis of bacterial fatty acids. Ozonolysis of unsaturated fatty acids as a means of determining the intramolecular distribution of carbon isotopes. Geochimica et Cosmochimica Acta 46, 139–149.

Morley, C., 1999. Comparison of hydrocarbon prospectivity in rift systems. In: Morley, C. (Ed.), Geoscience of Rift Systems-Evolution of East Africa. AAPG Studies in Geology, vol. 44, pp. 233–242.

Nguyen Tu, T., Kurschner, W., Schouten, S., Van Bergen, P., 2004. Leaf carbon isotope composition of fossil and extant oaks grown under differing atmospheric CO_2 levels. Palaeogeography Palaeoclimatology Palaeoecology 212, 199–213.

Niggemann, J., Schubert, C., 2006. Fatty acid biogeochemistry of sediments from the Chilean coastal upwelling region: sources and diagenetic changes. Organic Geochemistry 37, 626–647.

O'Leary, M., 1976. Carbon isotopic effect of the enzymatic decarboxylation of pyruvic acid. Biochemical and Biophysical Research Communications 73, 614–618.

O'Leary, M., 1981. Carbon isotope fractionation in plants. Phytochemistry 20, 553–567.

Partridge, T.C., Bond, G.C., Hartnandy, C.J.H., deMenocal, P.B., Ruddiman, W.F., 1995. Climatic effects of late Neogene tectonism and volcanism. In: Vrba, E., Denton, G., Burckle, L., Partridge, T. (Eds.), Paleoclimate and Evolution With Emphasis on Human Origins. Yale University Press, New Haven, pp. 8–23.

Pearson, A., Eglinton, T., 2000. The origin of *n*-alkanes in Santa Monica Basin surface sediment: a model based on compound-specific $\Delta^{14}C$ and $\delta^{13}C$ data. Organic Geochemistry 31, 1103–1116.

Pokras, E., Mix, A.C., 1987. Earth's precession cycle and Quaternary climatic change in tropical Africa. Nature 326, 486–487.

Prospero, J., Ginoux, P., Torres, O., Nicholson, S., Gill, T., 2002. Environmental characterization of global sources of atmospheric soil dust intentified with the Nimbus 7 Total Ozone Mapping Spectrometer (TOMS) absorbing aerosol product. Reviews of Geophysics, 40. doi:10.1029/2000RG00009.

Quade, J., Levin, N., Semaw, S., Stout, D., Renne, P., Rogers, M., Simpson, S., 2004. Paleoenvironments of the earliest stone toolmakers, Gona, Ethiopia. Geological Society of America Bulletin 116, 1529–1544.

Reddy, C., Eglinton, T., Palic, R., Benitez-Nelson, B., Stojanovic, G., Palic, I., Djordjevic, S., Eglinton, G., 2000. Even carbon number predominance of plant wax *n*-alkanes: a correction. Organic Geochemistry 31, 331–336.

Rieley, G., Collister, J., Stern, B., Eglinton, G., 1993. Gas chromatography/isotope ratio mass spectrometry of leaf wax *n*-alkanes from plants of differing carbon dioxide metabolisms. Rapid Communications in Mass Spectrometry 7, 488–491.

Rogge, W., HIldemann, L., Mazurek, M., Cass, G., Simoneit, B., 1993. Sources of fine organic aerosol. 4. Particulate abrasion products from leaf surfaces of urban plants. Environmental Science and Technology 27, 2700–2711.

Rommerskirchen, F., Eglinton, G., Dupont, L., Gunter, U., Wenzel, C., Rullkötter, J., 2003. A north to south transect of Holocene southeast Atlantic continental margin sediments: relationships between aerosol transport and compound-specific $\delta^{13}C$ land plant biomarker and pollen records. Geochemistry Geophysics Geosystems 4, 1–29.

Rossignol-Strick, M., 1983. African monsoons, an immediate climatic response to orbital insolation forcing. Nature 304, 46–49.

Sarna-Wojcicki, A.M., Meyer, C.E., Roth, P.H., Brown, F.H., 1985. Ages of tuff beds at East African early hominid sites and sediments in the Gulf of Aden. Nature 313, 306–308.

Schefuss, E., Ratmeyer, V., Stuut, J.B.W., Jansen, J.H.F., Damsté, J.S.S., 2003a. Carbon isotope analyses of *n*-alkanes in dust from the lower atmosphere over the central eastern Atlantic. Geochimica et Cosmochimica Acta 67, 1757–1767.

Schefuss, E., Schouten, S., Jansen, J.H.F., Damsté, J.S.S., 2003b. African vegetation controlled by tropical sea surface temperatures in the mid-Pleistocene period. Nature 422, 418–421.

Schefuss, E., Schouten, S., Schneider, R., 2005. Climatic controls on central African hydrology during the past 20,000 years. Nature 437, 1003–1006.

Scholz, C., King, J., Ellis, G., Swart, P., Stager, J.C., Colman, S., 2003. Paleolimnology of Lake Tanganyika, East Africa over the past 100kyr. Journal of Paleolimnology 30, 139–150.

Schulze, E.D., Ellis, R., Schulze, W., Trimborn, P., Ziegler, H., 1996. Diversity, metabolic types and delta^{13}C carbon isotope ratios in the grass flora of Namibia in relation to growth form, precipitation and habitat conditions. Oecologia 106, 352–369.

Simoneit, B., 1997. Compound-specific carbon isotope analyses of individual long-chain alkanes and alkanoic acids in Harmattan aerosols. Atmospheric Environment 31, 2225–2233.

Street-Perrott, F.A., Ficken, K.J., Huang, Y., Eglinton, G., 2004. Late Quaternary changes in carbon cycling on Mt. Kenya, East Africa: an overview of the $\delta^{13}C$ record in lacustrine organic matter. Quaternary Science Reviews 23, 861–879.

Tiedemann, R., Sarnthein, M., Shackleton, N.J., 1994. Astronomical timescale for the Pliocene Atlantic $\delta^{18}O$ and dust flux records of ODP Site 659. Paleoceanography 9, 619–638.

Tissot, B., Welte, D., 1984. Petroleum Formation and Occurrence. Springer-Verlag, Heidelberg.

Trauth, M., Deino, A., Strecker, M., 2001. Response of the East Africa climate to orbital forcing during the last interglacial (130–117 ka) and the early last glacial (117–60 ka). Geology 29, 499–502.

Tuenter, E., Weber, S., Hilgen, F., Lourens, L., 2003. The response of the African summer monsoon to remote and local forcing due to precession and obliquity. Global and Planetary Change 36, 219–235.

Volkman, J., Barrett, S., Blackburn, S., Mansolur, M., Sikes, E., Gelin, F., 1998. Microalgal biomarkers: a review of recent research developments. Organic Geochemistry 29, 1163–1179.

Volkman, J., Johns, R., Gillan, F., Perry, G., 1980. Microbial lipids of an intertidal sediment – 1. Fatty acids and hydrocarbons. Geochimica et Cosmochimica Acta 44, 1133–1143.

Walter, R.C., Aronson, J., 1993. Age and source of the Sidi Hakoma Tuff, Hadar Formation, Ethiopia. Journal of Human Evolution 25, 229–240.

Westerhausen, L., Poynter, J., Eglinton, G., Erlenkeuser, H., Sarnthein, M., 1993. Marine and terrigenous origin of organic matter in modern sediments of the equatorial East Atlantic: the $\delta^{13}C$ and molecular record. Deep-Sea Research 140, 1087–1121.

White, F., 1983. Vegetation of Africa – a descriptive memoir to accompany the Unesco/AETFAT/UNSO vegetation map of Africa. In: Natural Resources Research Report XX, U.N. Educational, Scientific and Cultural Organization, Paris.

White, T.D., Suwa, G., Hart, W., Walter, R.C., WoldeGabriel, G., de Heinzelin, J., Clark, J.D., Asfaw, B., Vrba, E., 1993. New discoveries of *Australopithecus* at Maka in Ethiopia. Nature 366, 261–265.

Wynn, J.G., 2004. Influence of Plio-Pleistocene aridification on human evolution: evidence from paleosols of the Turkana Basin, Kenya. American Journal of Physical Anthropology 123, 106–118.

Zhao, M.X., Dupont, L., Eglinton, G., Teece, M., 2003. *n*-Alkane and pollen reconstruction of terrestrial climate and vegetation for NW Africa over the last 160 kyr. Organic Geochemistry 34, 131–143.